Available online at www.sciencedirect.com

SciVerse ScienceDirect

Ceramics International 38 (2012) 4319–4323

CERAMICS INTERNATIONAL

www.elsevier.com/locate/ceramint

Comparative analysis of cadmium doped magnesium ferrite $Mg_{(1-x)}\,Cd_x\,Fe_2O_4$ ($x = 0.0, 0.2, 0.4, 0.6$) nanoparticles

Manpreet Kaur [a,*], Shweta Rana [b], P.S. Tarsikka [c]

[a] Department of Chemistry, Punjab Agricultural University, Ludhiana 141 004, India
[b] Department of Chemistry, Punjab University, Chandigarh 160014, India
[c] Department of Physics, Punjab Agricultural University, Ludhiana 141 004, India

Received 21 December 2011; received in revised form 2 February 2012; accepted 5 February 2012
Available online 13 February 2012

Abstract

Oxalyl dihydrazide–metal nitrate combustion route was employed to synthesize $Mg_{(1-x)}\,Cd_x\,Fe_2O_4$ ($x = 0.0, 0.2, 0.4, 0.6$) nanoparticles (NPs). Ferrite NPs were analyzed by various physico-chemical techniques viz. X-ray diffraction, scanning electron microscopy (SEM) and transmission electron microscopy (TEM). Vibrating sample magnetometer (VSM) was used to study effect of doping on the magnetic parameters of ferrite. Combustion method proved a low temperature route for preparation of mono disperse ferrite nanoparticles with average particle diameter of 22–34 nm. In the present study saturation magnetization and remnant magnetization increased with cadmium content up to $x = 0.4$, $Mg_{0.6}Cd_{0.4}Fe_2O_4$ showed promising magnetic and micro structural properties exploring its potentiality as soft magnetic material. The temperature of ferrite formation (300 °C) was much lower than the reported value (700 °C) for co-precipitation method. This can be attributed to the fact that intimate mixing of cations and exothermic decomposition of combustion mixture facilitates solid state reaction and stabilization of metastable phases thus lowering the external temperature required for ferrite formation. Another advantage of combustion approach is that it does not involve sintering and milling at elevated temperature (as required in conventional ceramic method) which introduces lattice defects, strains and causes coarsening of ferrite. In the present case high purity products with desired stoichiometry and promising magnetic properties were obtained.

Keywords: D. Ferrite; Combustion; X-ray diffraction; Hysteresis; TEM

1. Introduction

Spinel ferrites have received appreciable interest owing to their promising magnetic properties and are extensively used in microwave devices, ferrofluids, ferroseals and memory cores of computers. [1–6] Magnesium ferrite is widely applicable soft magnetic material for transformer cores, humidity sensors and catalysis [7–9]. AB_2O_4 is a general formula for spinels where tetrahedral A sites and octahedral B sites are occupied by metal cations. Magnetic properties of ferrites can be suitably tailored by varying composition of cations. Doping of ferrite with small amount of non magnetic ions such as Zn^{2+} or Cd^{2+} results in augmentation of saturation magnetization [10]. Conventional ceramic method is most common commercial approach for bulk syntheses of ferrites but it suffers severe drawback of high temperature milling and sintering which in turn yields inhomogeneous and coarse products. Moreover, milling introduces lattice defects and strains in ferrites. Soft chemical routes such as co-precipitation, precursor and combustion approach are gaining interest of scientific community as they have an edge over conventional ceramic method in the syntheses of nanophase ferrites with improved properties [11–20]. Yang and Yen [19] synthesized Zn ferrite nanopowders via precursor route and reported the formation of single phase ferrite by annealing treatment to precursor powder at 350 °C. Lakeman and Payne have reviewed sol–gel processing to synthesize variety of oxides and ferrites [20]. Whereas Cd doped magnesium ferrites have also been prepared using co-precipitation process by Gadkari et al. [11] but major constrain of this method include incomplete precipitation and quite high (700 °C) temperature of ferrite formation. On the contrary, combustion and precursor routes involve intimate molecular level mixing of metal ions and yield products with desired stoichiometery and high

* Corresponding author. Tel.:+91 8146200711.
E-mail address: manpreetchem@pau.edu (M. Kaur).

0272-8842/$36.00
doi:10.1016/j.ceramint.2012.02.013

surface area. In precursor approach synthesis and thermolysis of ferricarboxylate precursor is employed to synthesize ferrite nanoparticles. In combustion synthesis exothermicity of redox reaction mixture is used to produce useful materials [13]. Rapid oxidative pyrolysis of the combustion mixture is catalyzed in the presence of carbohydrazide/oxalyl dihydrazide/glycine/polyacrylic acid etc. which act as fuel and lower the external temperature required for solid state reaction hence provide low temperature route for obtaining voluminous and large surface area ferrite nanoparticles. Stoichiometrically pure and crystalline ferrite nanoparticles have already been prepared by precursor and combustion methods. But there seems no work on synthesis of Cd doped magnesium ferrites by these methods.

The present work was undertaken to synthesize of Cd doped magnesium ferrite $Mg_{(1-x)}Cd_xFe_2O_4$ by combustion method and to investigate the effect of preparative method and stoichiometery on magnetic properties in comparison with co precipitation method.

2. Experimental

Following chemicals (AR grade) were used without further purification. The source is given in the parenthesis:

$Mg(NO_3)_2$ (s.d fine Chemicals), $Cd(NO_3)_2$ (Loba Chem) $Fe(NO_3)_3$ (Loba Chem), diethyl oxalate(Qualigens), Hydrazine hydrate (Loba Chem).

2.1. Synthesis of oxalyl dihydrazide (ODH)

Oxalyl dihydrazide (ODH) was prepared by dropwise addition of 1 mol of diethyl oxalate in 2 mol of hyrdrazine hydrate at 273 K with constant stirring. White precipitates of ODH obtained were washed with cold water and stored in a vacuum desiccator. The identity of oxalyl dihydrazide was established by elemental analysis and mass spectroscopy.

2.2. Synthesis of ferrites from ODH-metal nitrates

For the synthesis of ferrites stoichiometric aqueous solutions of metal nitrates were mixed with ODH in silica crucible. The reaction mixture was heated in a muffle furnace at 300 °C. The reaction was rapid and combustion process was over in 15 min. The final product was sintered at 300 °C for 3 h. Syntheses of ferrites by redox reaction is represented in Scheme 1.

2.3. Characterization techniques

XRD powder pattern were recorded in Paranalytical expert pro mpt 2007 instrument using nickel filtered Cu-K_α radiation.

$$\begin{aligned}(1-x)Mg(NO_3)_2(aq) + xCd(NO_3)_2(aq) \\ + 2Fe(NO_3)_3(aq) + 4\,C_2H_6N_4O_2 \\ \rightarrow Mg_{(1-x)}Cd_x\,Fe_2O_4 + 8CO_2 + 12\,N_2 + 12H_2O\end{aligned}$$

Scheme 1.

Scanning electron micrographs (SEM) were recorded employing Hitachi-S-3400N scanning electron microscope at 15.0–20 kV acceleration voltage in SE mode The sputtering was performed by E-1010 Ion sputter coater to obtain a gold layer of 10–20 nm thickness. Transmission electron micrographs (TEM) of end products were recorded by employing Transmission Electron Microscope model Hitachi Hi-7650 at 100 kV acceleration voltage in HC mode using water as a dispersion medium. The TEM processing involved drop method technique on carbon coated 200 mesh size copper grid. The grid was later on air dried. The magnetic properties of ferrite powder samples were studied by employing vibrating sample magnetometer Model PAR-155 Germany.

3. Results and discussion

3.1. Physical density

Physical densities of the samples were evaluated by Archimedes principle with pyknometer employing xylene as a medium [21]. On increasing the Cd content an increase in physical density was observed from 4.127 g/cc to 4.637 g/cc (Table 1). This is attributed to the fact that mass volume ratio of Cd is greater than the mass volume ratio of Mg. Doping of Zn ions has also been reported to cause similar densification and grain growth [22].

3.2. XRD studies

X-ray diffraction (XRD) displayed sharp peaks (Fig. 1) which clearly reveal the formation of well-crystalline single phase magnesium ferrite [23]. Lattice constant (a) was calculated using the most intense (3 1 1) XRD peak using equation:

$$a = d(h^2 + k^2 + l^2)^{1/2}$$

The XRD density was calculated by formula [23]:

$$\text{Density} = \frac{8M}{Na^3}$$

where M is molecular weight of the sample and N is Avogadro's number.

X-ray density also exhibited escalating trend on increasing cadmium content but the values were higher than corresponding physical densities. The lower values in later case can be attributed to the porosity of the powder samples. The percentage porosity for all the compositions was calculated by using equation [24]:

$$\left[\frac{1 - d_{\exp}}{d_{\mathrm{XRD}}}\right] \times 100$$

Results of XRD studies revealed that the porosity values vary with different compositions (Table 1). Low value of percentage porosity is the essential requirement for a good quality material. On the other hand, larger magnitude of

Table 1
XRD parameters of the $Mg_{(1-x)}$ Cd_x Fe_2O_4 ($x = 0.0$–0.6) ferrites.

Cd^{2+}	Lattice constant (Å)	X-ray density (g/cc)	Physical density (g/cc)	%Age porosity	Average particle diameter(nm)
0.0	8.4597	4.387	4.127	5.93	80 ± 3.2
0.2	8.4604	4.775	4.396	7.94	65 ± 2.1
0.4	8.4706	5.144	4.532	11.90	53 ± 2.5
0.6	8.5423	5.393	4.735	14.02	44 ± 4.1

porosity deteriorates the magnetic and elastic behaviour of the material even at low frequency region.

Average particle size (D) was calculated using Scherrer's relationship [25]:

$$D = \frac{\lambda}{d\cos\theta}$$

where d is full width at half maximum. X-ray density values were lower than the reported values for cadmium doped magnesium ferrites prepared by co-precipitation method [11] as in the later route higher temperature requirement resulted in densification of the ferrite phase. The value of D decreases from 80 nm to 44 nm on increasing value of x. This can be attributed to the liberation of latent heat at the surface which raises the local temperature, consequently slowing down the growth process and lowering ferrite concentration in the vicinity [26].

3.3. Micro structural studies

Surface morphology of the sample $Mg_{(1-x)}$ Cd_x Fe_2O_4 ($x = 0.0$) as observed by SEM picture as shown in Fig. 2 revealed particle aggregation indicating that magnetic nanoparticles tend to form clusters and aggregates in powder form. These individual particles could not be resolved by SEM. The sizes of agglomerates vary from 12 to 20 μm. On the contrary TEM images taken by water dispersion method at high and low magnification in Fig. 3(a)–(c) clearly revealed ultra fine, well dispersed spherical ferrite nanoparticles with average particle diameter of 34 ± 2.7 nm. Similar correlation between TEM and SEM results of lead selenide nanoparticles is also reported [27]. The particle size distribution histogram (Fig. 3d) was prepared by the method reported by Bakshi [28] shows that maximum fraction of particles have size between 20 and 30 nm,Other samples displayed small decrease with increasing Cd content with the minimum value of 22 ± 4.2 nm for $x = 0.6$. The particle size calculated by XRD line broadening varies from the microscopic investigations. In XRD the calculations were done theoretically where as SEM and TEM images gave actual pictorial morphological characteristics of ferrite nanoparticles.

3.4. Magnetic studies

VSM results revealed effect of varying stoichiometery on magnetic parameters of the ferrite samples (Table 2). Hysteresis plots showing the variation of magnetization (M, emu/g) as a function of applied magnetic field (H, Oe) were plotted for prepared ferrite samples (Fig. 4). All the samples displayed normal (s shaped) narrow hystersis loops. Magnetic parameters like saturation magnetization (M_s), remanent magnetization (M_r) and coercivity (H_c) of the samples were compared which in turn depend upon number of factors viz. density, anisotropy, grain growth and A–B exchange interactions. Magnetic properties of these ferrite nanoparticles are of immense interest for the fundamental understanding of magnetic interactions and have great significance owing to their technological applications. Narrow loop indicated low coercivity values ranging from 60.5 Oe to 216.5 Oe. Low coercivity indicates that the prepared sample can be demagnetized easily which is an important requirement for a good electromagnet. Pure

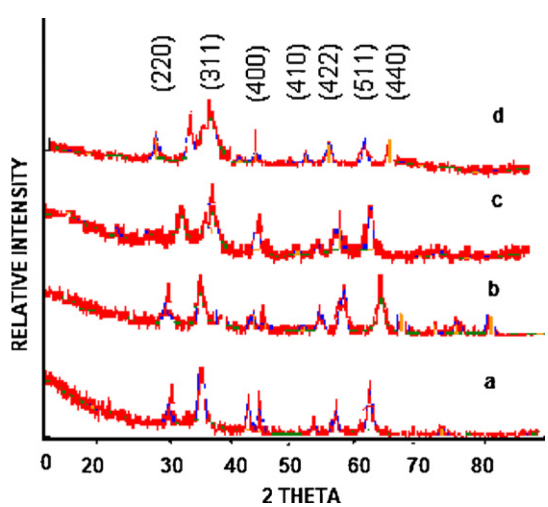

Fig. 1. XRD powder pattern of $Mg_{(1-x)}$ Cd_x Fe_2O_4 ($x = 0.0$–0.4) ferrites Values of x varying for a–d from 0.0, 0,2, 0.4 and 0.6 respectively.

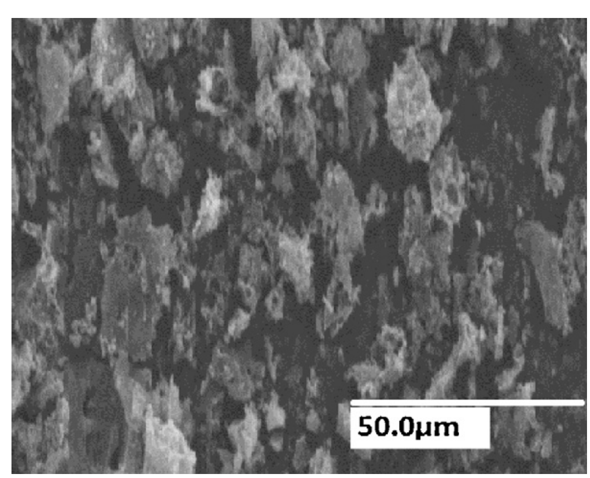

Fig. 2. Scanning electron micrograph for $MgFe_2O_4$.

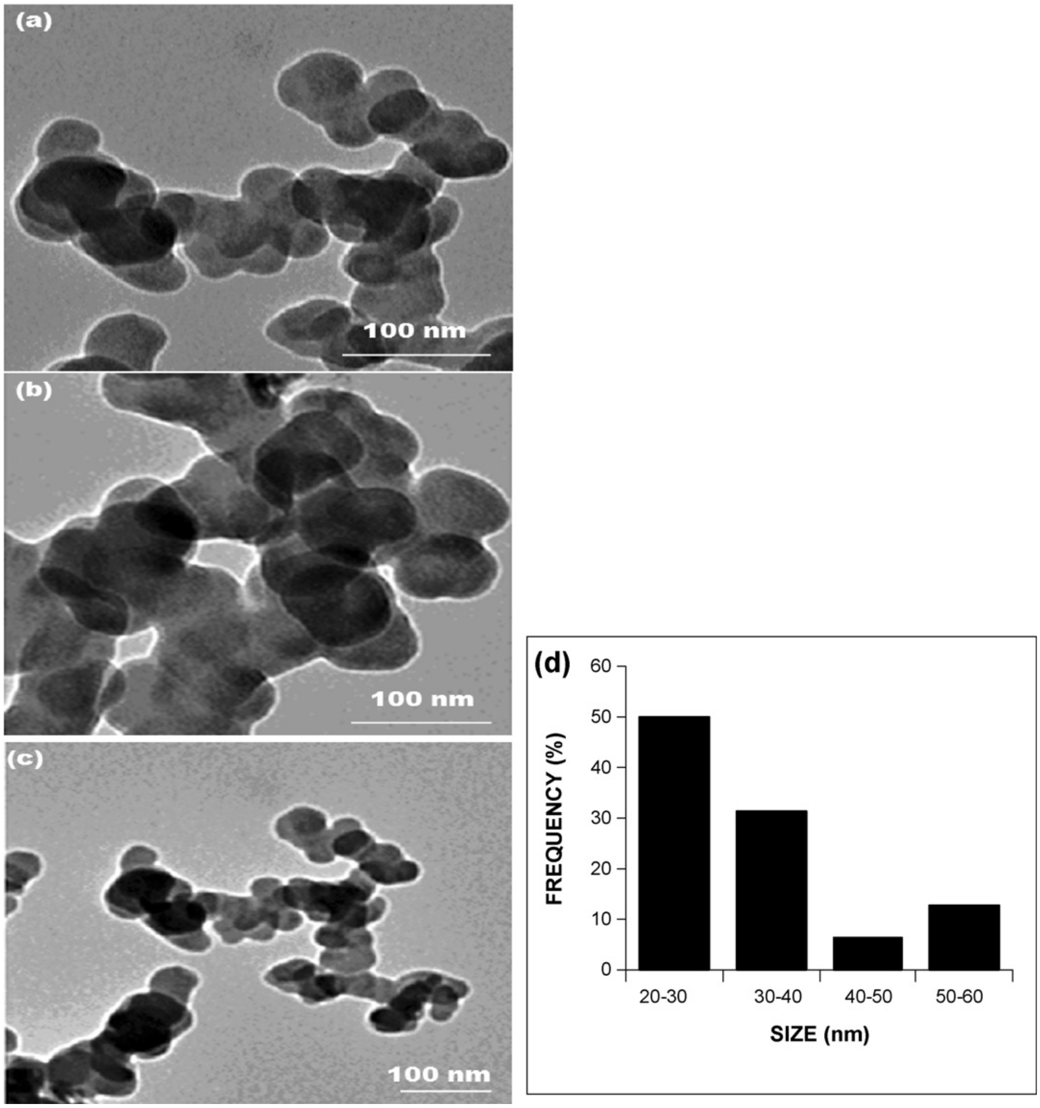

Fig. 3. (a)–(c) Transmission electron micrographs at high and low magnifications and (d) histogram showing particle size distribution.

magnesium ferrite displayed M_s M_r and H_c values of 13.24 emu/g, 1.27 emu/g and 82.4 Oe respectively. On increasing the Cd^{2+} content up to 0.4 there was enhancement in M_s of the samples. Cadmium doped Ferrite with composition $Mg_{0.6}Cd_{0.4}Fe_2O_4$ displayed the values of M_s and M_r 23.50 emu/g and 4.51 emu/g respectively. Increase in saturation magnetization at this stage can be attributed to Neel's theory of ferrimagnetism. For small concentration of non magnetic ions, saturation magnetization is represented by the relationship

$$M_s = |M_B - M_A|$$

where M_B and M_A denote magnetization of A and B site ions respectively. Increase in saturation magnetization on doping up to $x = 0.4$ is attributed to the non magnetic nature of Cd^{2+} ions. Due to their large ionic diameter Cd^{2+} ions prefer tetrahedral sites thereby lowering M_A and consequently enhancing the saturation magnetization. On the contrary high concentration of non magnetic Cd^{2+} ions in A site causes weakening of A–B interactions. Weaker coupling causes subsequent lowering of anisotropic energy and saturation magnetization as is observed on increasing x to 0.6.

Table 2
Magnetic parameters of the $Mg_{(1-x)}$ Cd_x Fe_2O_4 ($x = 0.0$–0.4) ferrites.

Cd^{2+} content	Saturation magnetization (emu/gm)	$4\pi M_s$ (gauss)	Coercivity (Oe)	Remnant magnetization (emu/gm)
0.0	13.24	166.43	82.4	1.27
0.2	13.25	166.55	216.5	2.50
0.4	23.50	295.40	166.7	4.51
0.6	16.30	204.89	60.5	0.93

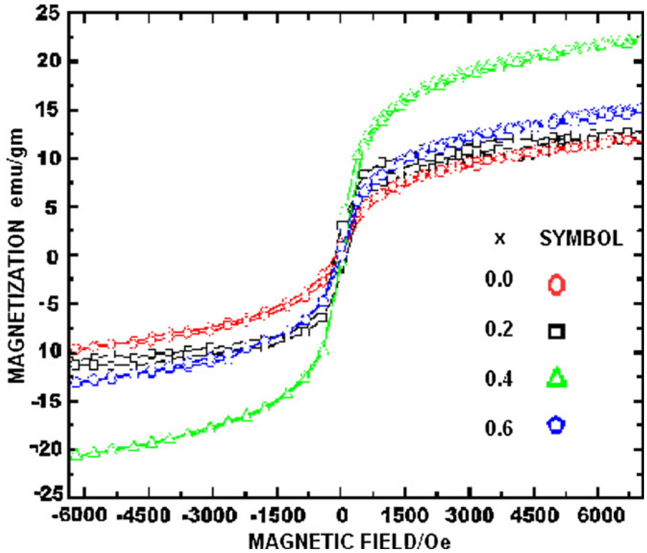

Fig. 4. Magnetic hysteresis for $Mg_{(1-x)}$ Cd_x Fe_2O_4 (x = 0.0–0.4) ferrites.

4. Conclusion

Oxalyl dihydrazide–metal nitrate combustion route provides a novel low temperature route for preparation of mono disperse ferrite nanoparticles with average particle size 22–30 nm. In the present study saturation magnetization and remnant magnetization increased with increasing Cd content up to $x = 0.4$, $Mg_{0.6}Cd_{0.4}Fe_2O_4$ displayed promising magnetic and micro structural properties indicating its potential as soft magnetic material. The temperature of ferrite formation (300 °C) was much lower than the reported value (700 °C) for co-precipitation method [11]. This can be attributed to the fact that intimate mixing of cations and exothermic decomposition of combustion mixture facilitates solid state reaction and stabilization of metastable phases which causes lowering of the external temperature required for ferrite formation. Another advantage of combustion approach is the avoidance of sintering and milling at elevated temperature (as required in conventional ceramic method) which introduces lattice defects, strains and causes coarsening of ferrite. In the present study high purity products with desired stoichiometery and promising magnetic properties were obtained.

References

[1] J.D. Adams, L.E. David, G.F. Dionne, E.F. Schloemann, S. Stizer, Ferrite devices and materials, IEEE Trans. Microw. Theory Technol. 50 (2002) 721–737.
[2] K. Raj, R. Maskowittz, R. Caseiari, Advances in ferrofluid technology, J. Magn. Magn. Mater. 149 (1995) 174–180.
[3] M.P. Horwath, Microwave applications of soft ferrites, J. Magn. Magn. Mater. 215 (2000) 171–183.
[4] U. Hafeli, W. Schitt, J. Teller, M. Zborowski, Scientific Clinical Applications of Magnetic Carriers, Plenum Press, New York, 1997.
[5] M.A. Willard, Y. Nakamura, E.D. Laughlin, M. Mc Henry, Magnetic properties of ordered and disordered spinel phase ferrimagnets, J. Am. Ceram. Soc. 82 (1999) 3342–3346.
[6] S.W. Charles, R. Chandershekkar, K.O. Geady, M. Walker, Ionic magnetic fluids based on cobalt ferrite nanoparticles, J. Appl. Phys. 64 (1988) 5840–5844.
[7] A.R. West, Basic Solid State Chemistry, 2nd ed., John Wiley and Sons Ltd., New York, 1988.
[8] R.K. Kotnala, J. Shah, M.C. Mathpal, D. Gupta, L.P. Purohit, H. Kishan, Role of modified active surface sites of magnesium ferrite for humidity sensing, J. Optoelect. Adv. Mater. 11 (2009) 296–301.
[9] G. Busca, E. Finocchio, V. Lorenzelli, M. Trombetta, S.A. Rossini, IR study of alkene allylic activation on magnesium ferrite and alumina catalysts, J. Chem. Soc., Faraday Trans. 92 (1996) 4687–4693.
[10] B. Viswanathan, V.R.K. Murthy, Ferrite materials, Narosa Publ. (1990), p. 11.
[11] A.B. Gadkari, T.J. Shinde, P.N. Vasambekar, Structural and magnetic properties of nanocrystalline Mg–Cd ferrites prepared by oxalate co-precipitation method, J. Mater. Sci. – Mater. Electron. 20 (2010) 96–103.
[12] A. Chatterjee, D. Das, S.K. Pradhan, D. Chakravorty, Synthesis of nanocrystalline nickel zinc ferrite by the sol–gel method, J. Magn. Magn. Mater. 127 (1993) 214–218.
[13] K.C. Patil, S.T. Aruna, T. Mimani, Combustion synthesis:an update, Curr. Opin. Solid State Chem. 6 (2002) 507–512.
[14] B.S. Randhawa, H.S. Dosanjh, M. Kaur, Preparation of spinel ferrites by citrate precursor route – a comparative study, Ceram. Int. 35 (2009) 1045–1049.
[15] J. Singh, H. Kaur, M. Kaur, B.S. Randhawa, Preparation of copper ferrites from thermolysis of copper tris(malonato)ferrate, J. Appl. Phys. 107 (2010) 520.
[16] B.S. Randhawa, M. Gupta, M. Kaur, Synthesis of cobalt ferrite from thermolysis of cobalt tris (malonato) ferrate(III) trihydrate precursor, Ceram. Int. 35 (2009) 3521–3524.
[17] B.S. Randhawa, M. Kaur, Application of Mossbauer spectroscopy to the thermal decomposition of strontium and barium bis(citrate) ferrates (III), Hyperfine Interact. 188 (2009) 95–101.
[18] B.S. Randhawa, H.S. Dosanjh, M. Kaur, Preparation of ferrites from combustion of metal nitrate-oxalyldihydrazide solutions, Ind. J. Eng. Mater. Sci. 12 (2005) 151–154.
[19] J.M. Yang, F.S. Yen, Evolution of intermediate phases in the synthesis of zinc ferrite nanopowders prepared by tartarate precursor method, J. Alloys Compd. 450 (2008) 387–394.
[20] C.D.E. Lakeman, D.A. Payne, Sol–gel processing of electric and magnetic ceramics, Mater. Chem. Phys. 38 (1994) 305–324.
[21] H.P. Klug, I. Alexander, X-Ray Diffraction Procedure, New York, 1962.
[22] N. Yahya, M.N. Arpin, A.A. Aziz, H. Daud, H.M. Zaid, L.K. PAL, N. Mauf, Synthesis and characterization of magnesium zinc ferrite as electromagnetic source, Am. J. Eng. Appl. Sci. 1 (2008) 53–58.
[23] ASTM Card No. 17–484.
[24] J. Smith, H.P.T. Wijn, N.N. Phillip, G. Eindhoven, Ferrites (Holland), 144A, 1959.
[25] E. Warren, X-Ray Diffraction, Addison Willey, Reading, 1969; R.F. Strickland-Constable, Kinetics and Mechanism of Crystallization, Academic Press, New York, 1968.
[26] R.F. Strickland-Constable, Kinetics and Mechanism of Crystallization, Academic Press, New York, 1968.
[27] M.S. Bakshi, V.S. Jaswal, G. Kaur, T.W. Simpson, P.K. Benipal, T.S. Benipal, F. Possmayer, N.O. Peterson, Biomineralization of BSA-Chalcogenide Nano and microcrystals, J. Phys. Chem. 113 (2009) 9121–9127.
[28] M.S. Bakshi, A simple method of superlattice formation step by step evaluation of crystal growth of gold nanoparticles through seed growth method, Langmuir 25 (2009) 12697–12705.